Supplementary Information

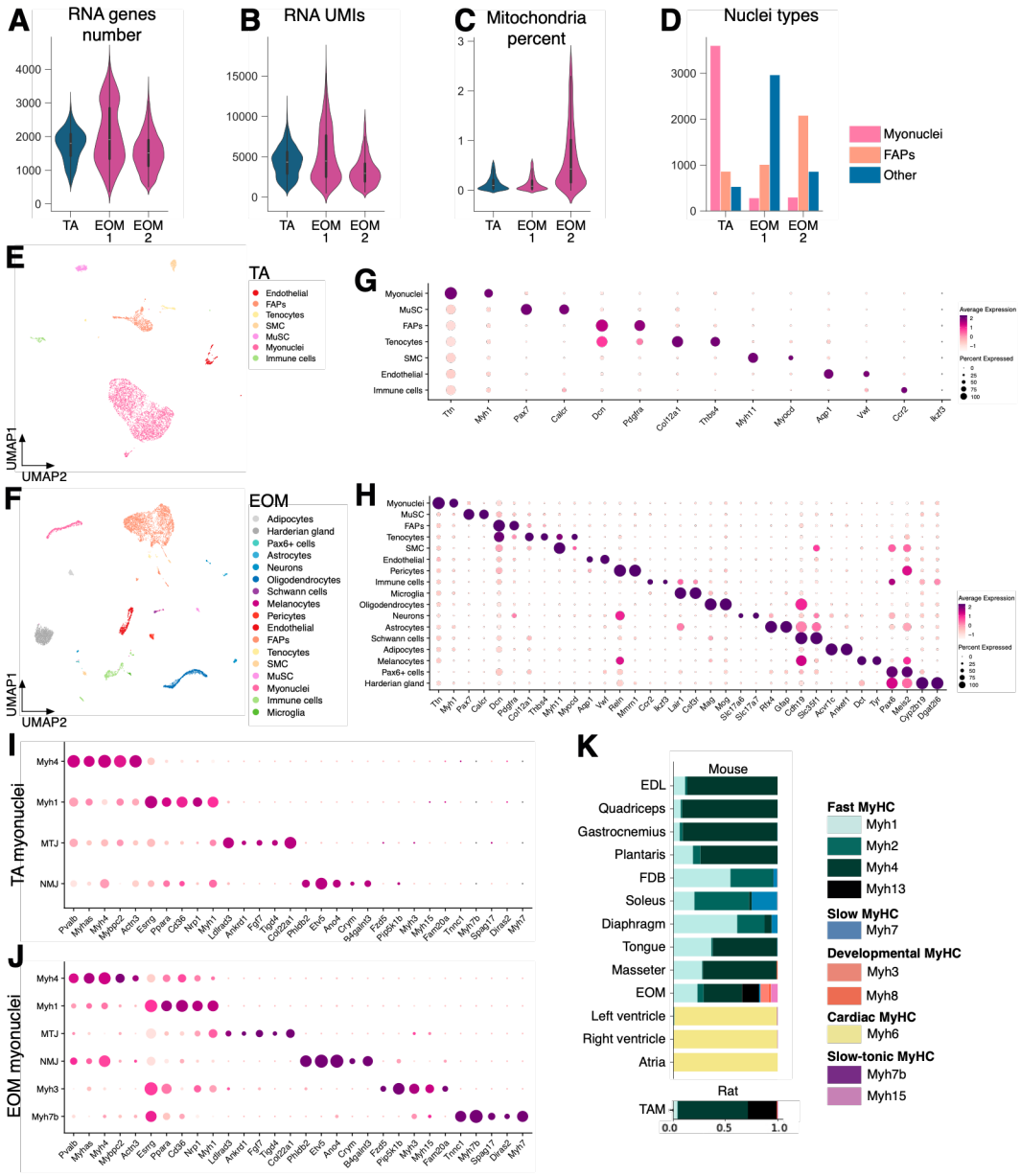
Myosin-binding protein composition tunes superfast contractility in vertebrates

The PDF file includes:

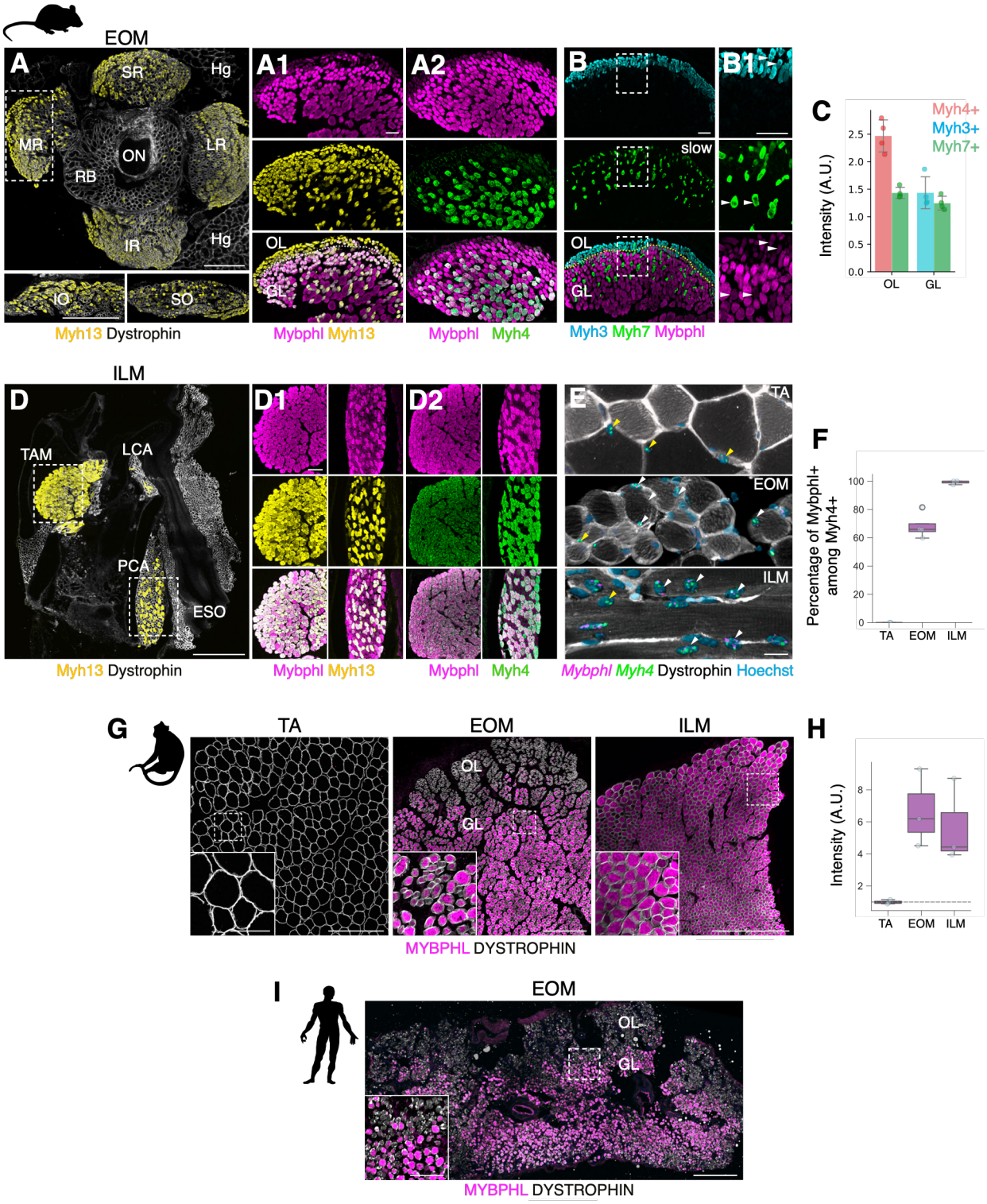
Supplementary Fig. 1 to 8
Supplementary Tables 1 to 3

Other Supplementary Materials for this manuscript include the following (not in the PDF):

Extended Data Tables 1 to 5

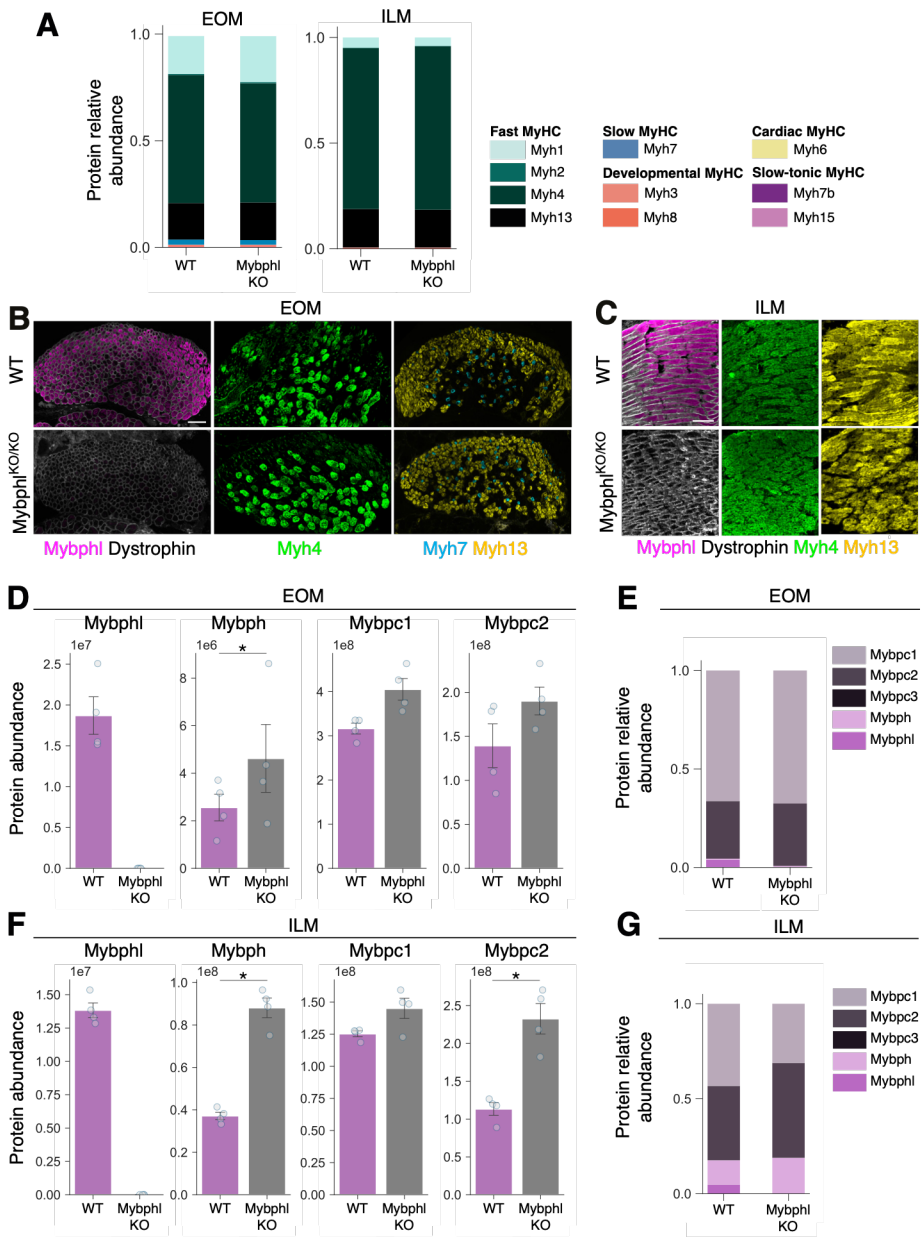


Suppl. Fig. 1. snRNA-seq analysis of EOM and TA. (A-B) Number of detected genes (A) and reads (B) per sample. (C) Percentage of reads of mitochondrial genes detected per nuclei. (D) Number of nuclei per cell type per sample after filtering. (E-F) Uniform manifold approximation and projection (UMAP) visualization of adult TA (E) and EOM (F) colored by cell type. Two independent EOM preparations were sequenced. (G-H) Dot plots of marker genes for each cell type in TA and EOM samples. (I-J) Dot plots of marker genes for each myonuclear subpopulation in TA (I) and EOM (J) samples. (K) Relative expression of myosin heavy chain (MyHC) transcripts among skeletal and cardiac mouse muscle tissues (re-analysis of (*21*)). EDL, extensor digitorum longus; EOM, extraocular muscles; FAPs, fibroadipogenic progenitors; FDB, flexor digitorum brevis; MuSC, muscle stem cells; SMC, smooth muscle cells; TA, tibialis anterior; UMIs, unique molecular identifiers.

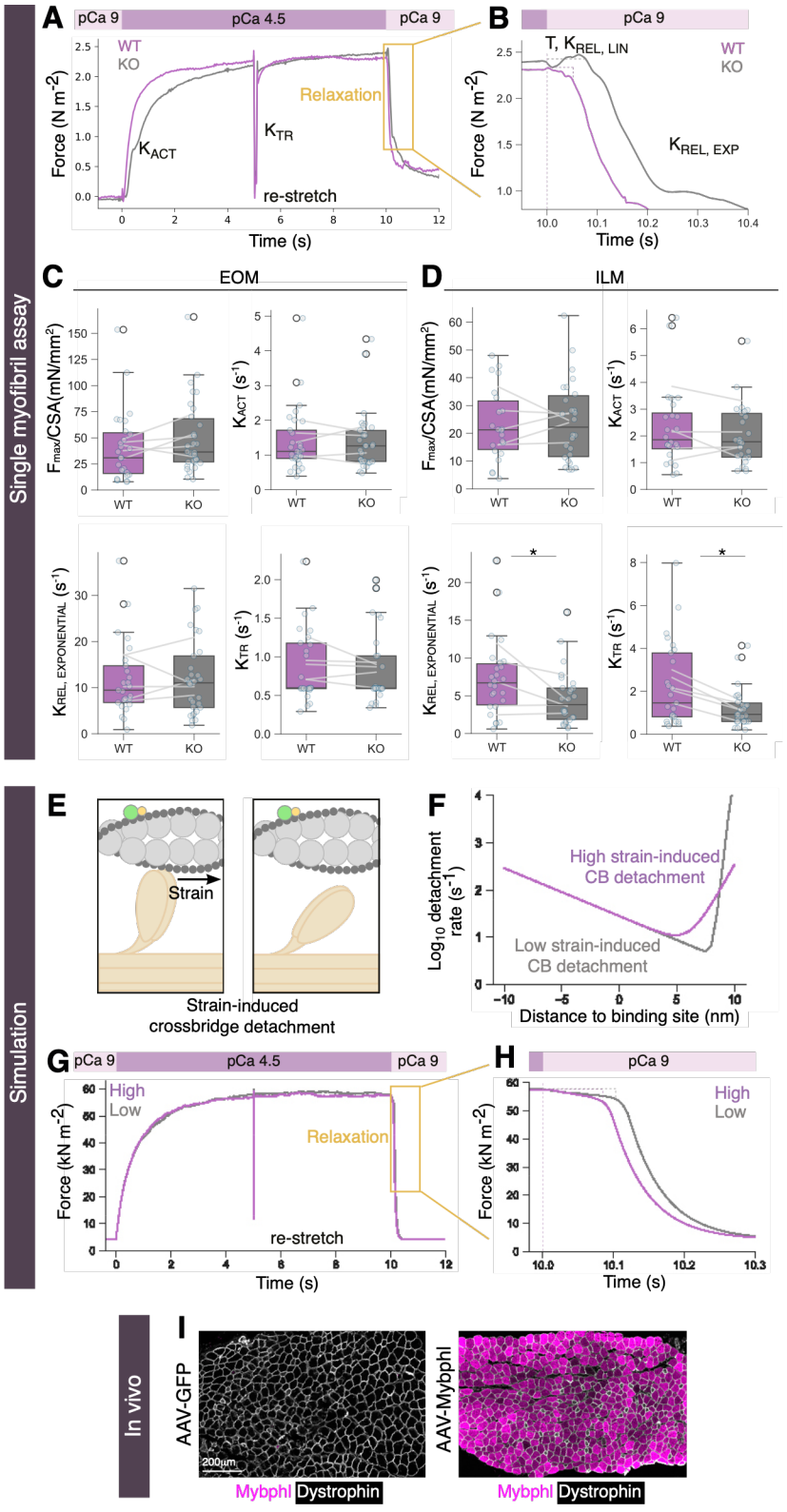


Suppl. Fig. 2. Mybphl expression across myofiber types. (A) Immunostaining of adult mouse EOM cryosections labelled with Myh13 and Dystrophin, Mybphl and Myh4. **(B)** Adult EOM muscle cryosections labelled with Myh3 (embryonic), Myh7 (slow fibres) and Mybphl. Higher magnification views in (B1) highlight mutually exclusive staining for Mybphl and Myh3/Myh7. The orbital layer (OL) and global layer (GL) are delimited with a yellow line. **(C)** Bar plot of intensity of fluorescence measurements of different

myosin heavy chain proteins (in arbitrary units, A.U) in the distinct EOM layers relative to TA intensity (set to 1). N=4 biological replicates. **(D)** Immunostaining of adult mouse ILM cryosections labelled with Myh13 and Dystrophin, Mybphl and Myh4. TAM and PCA as insets. **(E)** RNAscope using intronic probes for *Myh4* and *Mybphl* in adult TA, TAM and recti EOM. Dystrophin was used to label fiber membranes and nuclei stained with Hoechst and shown as iso-surfaces in Imaris. ILM (thyroarytenoid muscle) as longitudinal section, EOM and TA as cross-section. **(F)** Box plot of the percentage of *Mybphl*+ nuclei amongst all *Myh4*+ nuclei. N=3 biological replicates. **(G)** Immunostaining of adult *Macaca fascicularis* TA, EOM and TAM cryosections labelled with human Mybphl and Dystrophin antibodies. **(H)** Quantification of Mybphl intensity of fluorescence from the immunostainings in (G). N=3 female biological samples. **(I)** Immunostaining of adult human EOM cryosections labelled with human Mybphl antibody. N=2 biological replicates per group. CT, cricothyroid; EOM, extraocular muscles; ESO, esophagus striated muscle; GL, global layer; Hg, Harderian gland; IO, inferior oblique; IR, inferior rectus; LCA, lateral cricoarytenoid; ILM, intrinsic laryngeal muscles; LR, lateral rectus; MR, medial rectus; OL, orbital layer; ON, optic nerve; PCA, posterior cricoarytenoid muscle; RB, retractor bulbi; SO, superior oblique; SR, superior rectus; TA, tibialis anterior, TAM, thyroarytenoid muscle. Scale bars are 500μm in A, D, G, H, I; 100μm in A1, B, B1, D1; 15 μm in E, 250μm in insets in G, I.

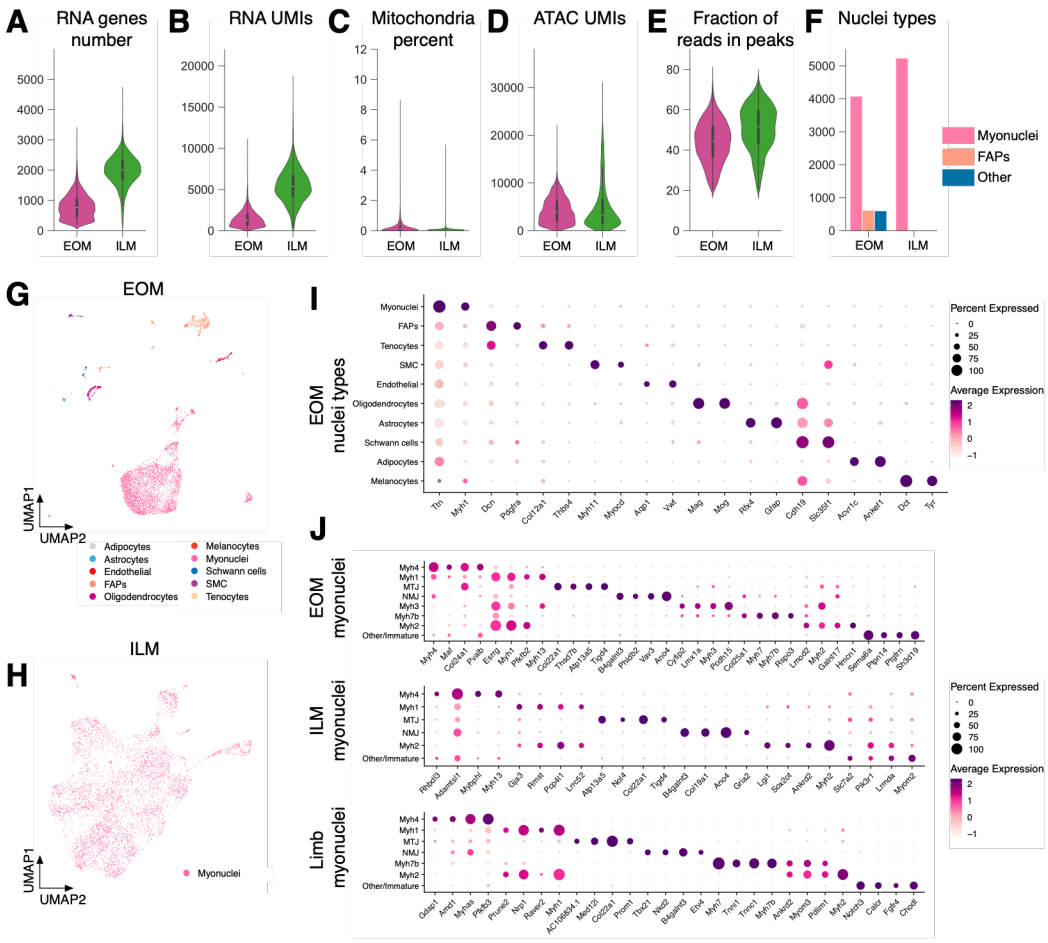


Suppl. Fig. 3. Molecular and histological characterisation of Mybphl knockout mice. (A) Relative abundance of myosin heavy chains (MyHC) proteins in adult wildtype (WT) and Mybphl$^{KO/KO}$ mouse EOM and ILM (thyroarytenoid muscle) by mass spectrometry-based proteomic analysis. **(B-C)** Immunostaining of adult WT and Mybphl$^{KO/KO}$ mouse EOM and ILM (thyroarytenoid muscle) cryosections labelled with the indicated antibodies. **(D)** MyBP abundance normalized on total MyHCs in EOM. Adjusted p-value=0.141 (Mybph), p-value=0.490 (Mybpc1), p-value=0.301 (Mybpc2). **(E)** Relative abundance of MyBPs in adult control and Mybphl$^{KO/KO}$ mouse EOM by mass spectrometry-based proteomic analysis. **(F)** MyBP abundance normalized on total MyHCs in ILM (thyroarytenoid muscle). Adjusted p-value=1.38e-9 (Mybph), p-value=0.613 (Mybpc1), p-value=5.45e-6 (Mybpc2). **(G)** Relative abundance of myosin binding proteins in adult WT and Mybphl$^{KO/KO}$ mouse EOM by mass spectrometry-based proteomic analysis. A, D-G, values are average of 4 biological replicates for each genotype. MyBP, myosin binding protein. Scale bars are 100µm in B,C.

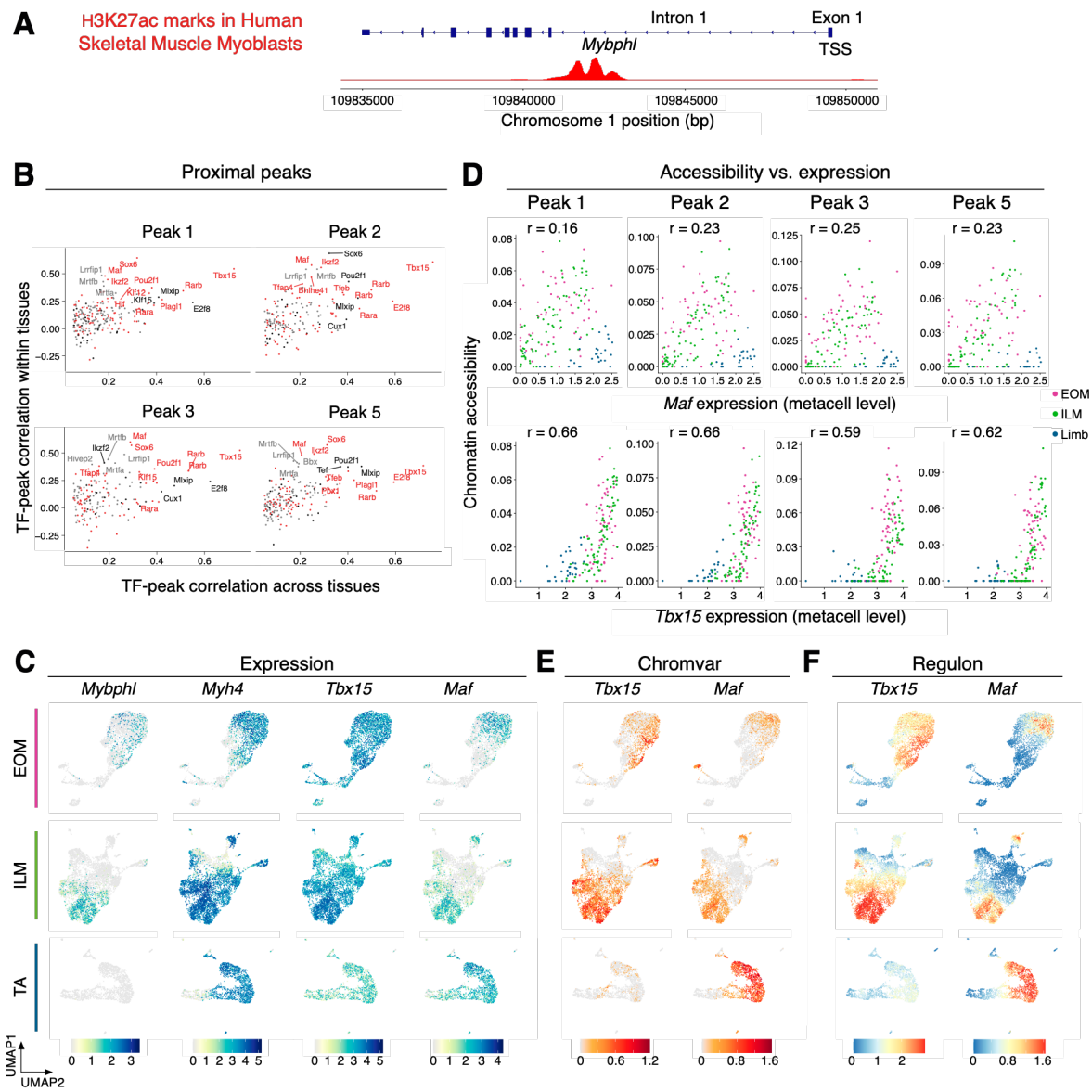


Suppl. Fig. 4. Experimental data and modeling of decreased strain-induced crossbridge detachment. **(A)** Trace of a representative single myofibril force measurement from wildtype (WT) or Mybphl$^{KO/KO}$ ILM (thyroarythenoid muscle). pCa changes correspond to force activation (k_{ACT}), redevelopment (k_{TR}) and

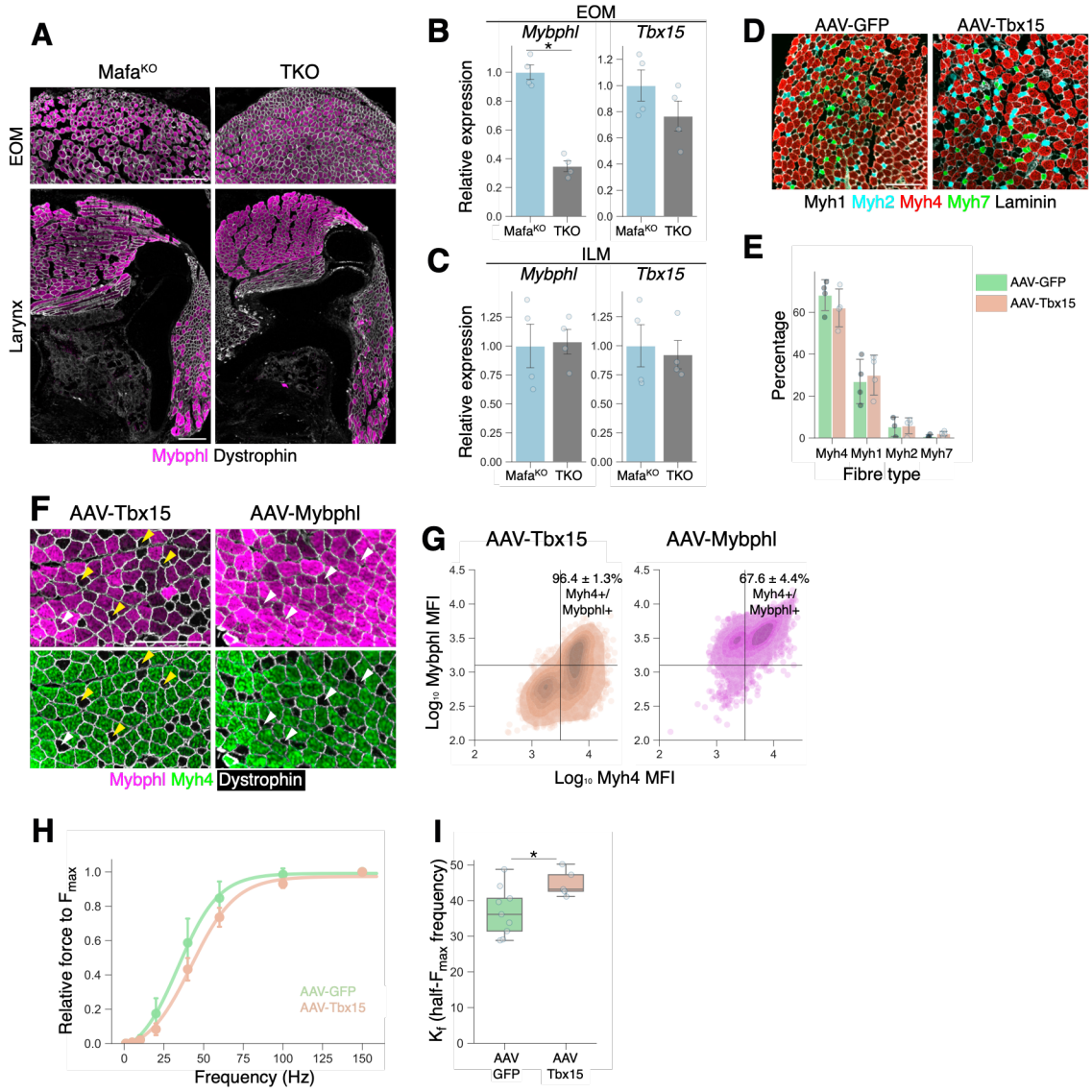
relaxation. **(B)** Expanded trace of the relaxation phase in A) composed of linear ($T,K_{REL,\ LIN}$) and exponential ($K_{REL,\ EXP}$) phases. **(C-D)** Quantification of single myofibril force measurements from EOM (N=5 for each group) and ILM (N=5 for each group). Linear mixed model was used with day of experiment as an independent random factor. For EOM, p-values = 0.292 (F_{MAX}), 0.976 (K_{ACT}), 0.801 (K_{EXP}), 0.587 (K_{TR}). For ILM, p-values = 0.886 (F_{MAX}), 0.333 (K_{ACT}), 0.013 (K_{EXP}), and 0.012 (K_{TR}). **(E)** Scheme of strain-induced crossbridge detachment. **(F)** Function of crossbridge detachment rate relative to the distance from actin binding site. **(G)** Trace of a simulated single myofibril force measurement with high and low strain-induced crossbridge detachment sensitivity. **(H)** Expanded trace of the relaxation phase in G). High strain-induced crossbridge detachment condition leads to shorter and more efficient relaxation while not affecting maximal force or other rate constants. **(I)** Immunostaining for Mybphl on EDL cryosections 3 weeks post post injection of AAV-Mybphl or AAV-GFP (control). Scale bar in I, 200μm.



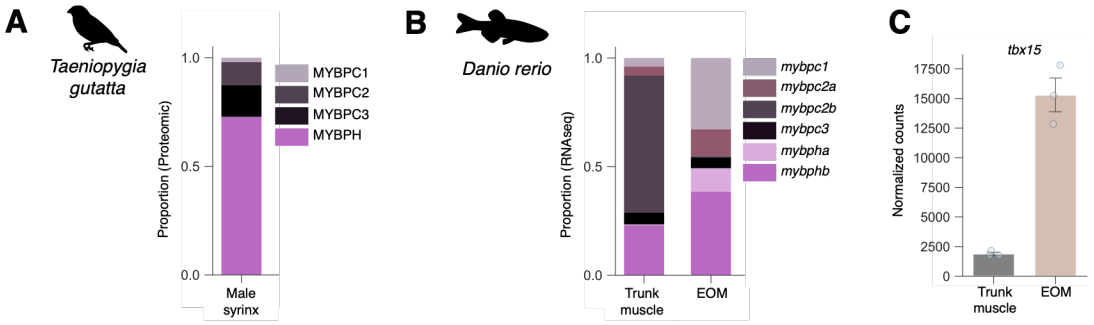
Suppl. Fig. 5. Multiome analysis of EOM and ILM. (A) Number of detected genes per sample using exonic and intronic sequences. **(B)** Number of gene expression reads per sample using exonic and intronic sequences. **(C)** Percentage of reads of mitochondrial genes detected per nuclei. **(D)** Number of ATAC-seq reads per sample. **(E)** Fraction of ATAC-seq reads in peaks per sample. **(F)** Number of nuclei per cell type per sample after filtering. **(G-H)** Uniform manifold approximation and projection (UMAP) visualization of EOM and ILM colored by cell type. **(I)** Dot plots of marker genes for each cell type in EOM. **(J)** Dot plots of marker genes for each myonuclear subpopulation in EOM and ILM samples. EOM, extraocular muscles; FAPs, fibroadipogenic progenitors; ILM, intrinsic laryngeal muscles; MTJ, myotendinous junction; NMJ, neuromuscular junction; SMC, smooth muscle cells, UMIs, unique molecular identifiers.



Suppl. Fig. 6. Inference of Mybphl regulators. (A) Track of ChIP-seq H3K27ac marks in human skeletal muscle myoblasts (ENCODE database). **(B)** Gene Regulatory Network inference of Mybphl regulators using Spearman correlation between transcription factor (TF) expression and chromatin accessibility at peaks 1, 2, 3, and 5, across tissues (trend over pooled metacells, global regulators) and within tissues (residual trend over each tissue's metacells, averaged, secondary regulators). **(C)** UMAP plot of RNA expression in all three datasets. (**D**) Correlation between expression of *Maf* (top lane) and *Tbx15* (bottom lane) and *Mybphl* peak 1, 2, 3 and 5 chromatin accessibilities. The Pearson correlation coefficient (r) is indicated on the plot. **(E-F)** UMAP plot of chromVAR score (E) and regulon score (F) in all three datasets.



Suppl. Fig. 7. Validation of Mybphl regulators. (A) Immunostaining of adult *Mafa*$^{KO/KO}$ and *Tg:HsaCre;Maf*$^{fl/fl}$*;Mafbfl*$^{fl/fl}$*;Mafa*$^{KO/KO}$ (TKO) EOM and ILM cryosections labelled with Mybphl antibody. **(B-C)** Relative expression levels of *Mybphl* and *Tbx15* by RT-qPCR in the same muscles as in (A). N=4 biological replicates per condition. Mann-Whitney U two-sided test, with p-value = 0.029 (*Mybphl*) and p-value = 0.343 (*Tbx15*) for EOM, and p-value = 0.886 (*Mybphl*), p-value = 0.886 (*Tbx15*) for ILM. **(D)** Immunostaining for Mybphl and the indicated myosin heavy chain antibodies on EDL cryosections 3 weeks post injection of AAV-Tbx15 or AAV-GFP (control). **(E)** Quantification of fiber type abundance in injected EDL muscles from (D). **(F)** Immunostaining for Mybphl and Myh4 on EDL cryosections 3 weeks post injection of AAV-Tbx15 or AAV-Mybphl. **(G-H)** Quantification of Mybphl abundance in Myh4-positive and negative fibers in (F). Note that almost all Mybphl-positive fibers are stained with Myh4 in the AAV-Tbx15 condition but not in the AAV-Mybphl condition. (**H**) Force-frequency curve of AAV injected EDL muscles. Force is relative to the maximal force elicited at 150 Hz. A sigmoid function is fitted on the mean points per condition. (**I**) Frequency eliciting half of the maximal force (K_f). N=9 AAV-GFP and N=5 AAV-Tbx15. Mann-Whitney U two-sided test with Benjamini-Hochberg correction with p-value = 0.0420. Same AAV-GFP control samples as in Figure 2I. EDL, extensor digitorum longus; EOM, extraocular muscles; ILM, intrinsic laryngeal muscles.



Suppl. Fig. 8. MyBP-H is expressed in vertebrate superfast muscles. (A) Relative abundance of myosin binding proteins in male zebra finch syrinx mass spectrometry based proteomics (reanalyzed from (*38*)). (**B**) Relative expression of myosin binding proteins in zebra finch bulk RNA-seq. N=3 for each group. (**C**) Expression levels of *Tbx15* in zebra finch bulk RNA-seq. Counts are displayed as Length-scaled Transcripts per Million based on Salmon output. EOM, extraocular muscles.

Line	Primer	Sequence
Mafa	Forward	TATGAGGCCTTCCGGGGTCAGAGCTTC
Mafa	Reverse (WT)	TCTGTTTCAGTCGGATGACCTCCTCCTTGC
Mafa	Reverse (KO)	CGATTGTCTGTTGTGCCCAGTC
Mafb flox	Forward	AGGTATGACTGTGTGGCT
Mafb flox	Reverse	CAAGCCAGAATGCAAAAGCG
Maf flox	Forward	AGACCACCTCAAGCAGGAGA
Maf flox	Reverse	GTTACGGGGGAATTCAGGTT
Cre(ACTA1cre)	Forward	GGACATGTTCAGGGATCGCCAGGCGT
Cre(ACTA1cre)	Reverse	GCATAACCAGTGAAACAGCATTGCTG
Mybphl KO	Forward	ACTGTAGGGATCAGGGTGGC
Mybphl KO	Reverse (WT)	ACCATACACCCATGCCCTTC
Mybphl KO	Reverse (KO)	TCGTGGTATCGTTATGCGCC
$R26^{H2BGFP}$	Forward (WT)	CTGGCTTCTGAGGACCG
$R26^{H2BGFP}$	Reverse (WT)	CAGGACAACGCCCACACA
$R26^{H2BGFP}$	Forward (KO)	ACCTCCAGGGAGATCCAGAC
$R26^{H2BGFP}$	Reverse (KO)	CTGAACTTGTGGCCGTTTAC
Tbx15 KO	Forward	TCTTCACAGGAGGATGTTTCC
Tbx15 KO	Reverse (KO)	GTCACGTTGGTGTAGATGGG
Tbx15 KO	Reverse (WT)	CCATTGGTGTATCCTCTGTCC

Suppl. Table 1.
List of primers used for genotyping

Target	Primer	Sequence
Tg_TBX15	Forward	CCAGCTTTGCAACCTCAACC
Tg_TBX15	Reverse	ATGAAGGTTTCGGAGGGCTG
Tg_MYBPC3	Forward	CACGCCAACTCAGACAGACT
Tg_MYBPC3	Reverse	TGCTGTTCCGAATTCCCACA
Tg_MYBPC1	Forward	ATGGAGGCACTTACACCTGC
Tg_MYBPC1	Reverse	TACCAGCTTCCAGTGCAGTG
Tg_MYBPC2	Forward	GAAGGGCGTCACCAAGAAGA
Tg_MYBPC2	Reverse	CTGCCCGTTCTTGTACCACT
Tg_MYBPH	Forward	ACAGCACTCACCTCTTCTGC
Tg_MYBPH	Reverse	CAGCCTTGCAGGTGTAGACA
Mm_Mybphl	Forward	TCACATCAACAGGAGGCAGG
Mm_Mybphl	Reverse	TGTAAGTCTGCTTCAGGGCC
Mm_Tbx15	Forward	TGTTCGCACACTGACCTTTG
Mm_Tbx15	Reverse	CCAGTGCTGGAGGTGGTT
Mm_Tbp	Forward	CAGCCTCAGTACAGCAATCAAC
Mm_Tbp	Reverse	TAGGGGTCATAGGAGTCATTGG

Suppl. Table 2.
List of primers used for RT-qPCR.

Reagent type or resource	Designation	Source or reference	Identifiers	Additional information
Strain (M.musculus)	B6D2F1/JRj	Janvier labs	/	
Strain (M.musculus)	B6.Cg-Tg(ACTA1-cre)79Jme/J	PMID: 10481039	MGI: 2447635	
Strain (M.musculus)	Mafa –/–	PMID: 15923615	MGI: 6324048	
Strain (M.musculus)	Mafb flox/flox	PMID: 27419056		
Strain (M.musculus)	Maf flox/flox	PMID: 31969519		
Strain (M.musculus)	Mybphl	PMID: 35533732	MGI: N/A	
Strain (M.musculus)	R26H2BGFP	PMID: 34616069	MGI: 6761491	
Strain (M.musculus)	Tbx15	PMID : 15652702	MGI: 3574402	
Antibody	Anti-alpha-actinin (Mouse monoclonal IgG1)	Sigma-Aldrich	Cat. #: A7811, RRID:AB_476766	IF (1:500)
Antibody	Anti-Dystrophin (Mouse monoclonal IgG2b)	DSHB	Cat. #: MANDYS8(8H11), RRID:AB_21477	IF (1:50)
Antibody	Alexa Fluor 405 F(ab')2 Fragment of Goat Anti-Rabbit IgG (H + L) (polyclonal antibody)	Life Technologies	Cat. #: A-31556, RRID:AB_221605	IF (1:500)
Antibody	Alexa Fluor 488 F(ab')2 Fragment of Goat Anti-Rabbit IgG (H + L) (polyclonal antibody)	Life Technologies	Cat. #: A-11070, RRID:AB_2534114	IF (1:500)
Antibody	Alexa Fluor 488 Goat Anti-Chicken IgG (H + L) (polyclonal antibody)	Life Technologies	Cat. #: A-11039, RRID:AB_2534096	IF (1:500)
Antibody	Alexa Fluor 555 F(ab')2 Fragment of Goat Anti-Rabbit IgG (H+L) (polyclonal antibody)	Life Technologies	Cat. #: A-21430, RRID:AB_2535851	IF (1:500)
Antibody	Alexa Fluor 633 F(ab')2 Fragment of Goat Anti-Rabbit IgG (H + L) (polyclonal antibody)	Life Technologies	Cat. #: A-21072, RRID:AB_2535733	IF (1:500)
Antibody	Alexa Fluor® 633 Goat Anti-Mouse IgG2b (γ2b) (polyclonal antibody)	Life Technologies	Cat. #: A-21146, RRID:AB_2535782	IF (1:500)
Antibody	Alexa Fluor® 647 anti-Nuclear Pore Complex Proteins Antibody	BioLegend	Cat. #:682204	Nuclei isolation (1:500)
Antibody	Alexa Fluor488 AffiniPure Goat Anti-Mouse IgG1 (γ1) (polyclonal antibody)	Jackson ImmunoResearch	Cat. #: 115-545-205, RRID:AB_2338854	IF (1:500)
Antibody	Anti-embryonic Myosin heavy chain, Myh3 (Mouse monoclonal IgG1)	DSHB	Cat. #: F1.652, RRID:AB_528358	IF (1:50)
Antibody	Anti-GFP (Chicken polyclonal)	Abcam	Cat# ab13970, RRID:AB_300798	IF (1:1000)
Antibody	Anti-Laminin (Rabbit polyclonal)	Sigma-Aldrich	Cat# L9393, RRID:AB_2618170	IF (1:1000)
Antibody	Anti-Mybphl (Rabbit polyclonal)	Barefield et al.,	/	IF (1:500)
Antibody	Anti-MYBPHL (Rabbit polyclonal)	Barefield et al.,	/	IF (1:500)
Antibody	Anti-Myh13	DSHB	Cat# 4A6, RRID:AB_528282	IF (1:50)
Antibody	Anti-Myh2	DSHB	Cat# SC-71, RRID:AB_2147165	IF (1:200)
Antibody	Anti-Myh4	DSHB	Cat# BF-23, RRID:AB_2266724	IF (1:200)
Antibody	Anti-Myh7	DSHB	Cat# BA-F8, RRID:AB_10572253	IF (1:200)
Antibody	Anti-Myh7	Sigma-Aldrich	Cat# MAB1628, RRID:AB_2282287	IF (1:500)
Antibody	Anti-PCM1 antibody produced in rabbit	Sigma-Aldrich	Cat. #:HPA023370	Nuclei isolation (1:500)
Antibody	Cy3-AffiniPure Goat Anti-Mouse IgG1 (γ1) (polyclonal antibody)	Jackson ImmunoResearch	Cat. #: 115-165-205, RRID:AB_2338694	IF (1:500)
Antibody	Goat anti-Mouse IgG1 Cross-Adsorbed Secondary Antibody, Alexa Fluor™ 633 - A-2112	Life Technologies	Cat. #: A-21126, RRID:AB_2535768	IF (1:500)
Antibody	Goat anti-Mouse IgG2b Cross-Adsorbed Secondary Antibody, Alexa Fluor™ 488 - A-211	Life Technologies	Cat. #: A-21141, RRID:AB_2535778	IF (1:500)
Antibody	Goat anti-Mouse IgM (Heavy chain) Cross-Adsorbed Secondary Antibody, Alexa Fluor™	Life Technologies	Cat. #: A-21426, RRID:AB_2535847	IF (1:500)
Antibody	Goat anti-Mouse IgM (Heavy chain) Secondary Antibody, Alexa Fluor™ 647 - A-21238	Life Technologies	Cat. #: A-21238, RRID:AB_2535807	IF (1:500)
Chemical compound, drug	1X DPBS without Ca2+/Mg2+	Gibco	Cat. #:14190-094	
Chemical compound, drug	Falcon™ Cell Strainers 40µm	Fischer Scientific	Cat. #:352340	
Chemical compound, drug	Falcon™ Cell Strainers 70µm	Fischer Scientific	Cat. #:352350	
Chemical compound, drug	Bovine Serum Albumin	Sigma-Aldrich	Cat. #:A9418	
Chemical compound, drug	BSA in 1X PBS	Sigma-Aldrich	Cat. #:A1595	
Chemical compound, drug	DTT	Sigma-Aldrich	Cat. #:646563	
Chemical compound, drug	Goat Serum	Sigma-Aldrich	Cat. #:11540526	
Chemical compound, drug	Hard Tissue homogenizing CK28 - Kit CK28 ceramid bead 2,8 mm, 2mL tube	Bertin	Cat. #:P000911-LYSK0-A	
Chemical compound, drug	HEPES pH 8.0	Invitrogen	Cat. #:H0887	
Chemical compound, drug	Hoechst 33342	Thermo Scientific	Cat. #:H3570	
Chemical compound, drug	Imalgene 1000	Boehringer	EAN #: 3661103003199	
Chemical compound, drug	Isopentane	VWR	Cat. #: 24872.298	
Chemical compound, drug	KCl	Sigma-Aldrich	Cat. #:P5405	
Chemical compound, drug	MgCl2	Sigma-Aldrich	Cat. #:M1028	
Chemical compound, drug	NaCl	Sigma-Aldrich	Cat. #:59222C-1000ML	
Chemical compound, drug	Nuclease-free Water	Invitrogen	Cat. #:AM9937	
Chemical compound, drug	Paraformaldehyde	Electron Microscopy Sciences	Cat. #: 15710	
Chemical compound, drug	PMSF	Sigma-Aldrich	Cat. #:P7626	
Chemical compound, drug	Protease inhibitor	Merck	Cat. #:11873580001	
Chemical compound, drug	Rompun 2%	Elanco	EAN #: 4007221032311	
Chemical compound, drug	RNAse Inhbitor	Roche	Cat. #:3335399001	
Chemical compound, drug	Sucrose, for molecular biology, ≥ 99.5%	Sigma-Aldrich	S0389-500G	
Chemical compound, drug	Tissue Tek OCT Compound	Sakura Finetek USA Inc	Cat. #: 4583	
Chemical compound, drug	Tris-HCl (pH 7.4)	Sigma-Aldrich	Cat. #:T2184-100ML	
Chemical compound, drug	Tris-HCl pH 8.0	Sigma-Aldrich	Cat. #:J22638.AE	
Chemical compound, drug	Triton X-100	Sigma-Aldrich	Cat. #: T8787	
Chemical compound, drug	Tween 20	Sigma-Aldrich	Cat. #: P1379	
Chemical compound, drug	Tween 20	Biorad	Cat. #:1610781	
Commercial assays	Agilent High Sensitivity DNA Kit	Agilent	Cat. #: 5067-4626	
Commercial assays	Agilent High Sensitivity DNA Reagents	Agilent	Cat. #: 5067-4627	
Commercial assays	Chromium Next GEM Chip G Single Cell Kit, 16 rxns	10X Genomics	Cat. #: 1000127	
Commercial assays	Chromium Next GEM Single Cell 3' GEM, Library & Gel Bead Kit v3.1, 4 rxns	10X Genomics	Cat. #: 1000128	
Commercial assays	NextSeq™ 500/550 High Output Kit v2.5	Illumina	Cat. #: 20024906	
Commercial assays	Qubit dsDNA HS Assay Kit	Life Technologies	Cat. #: Q32854	
Commercial assays	RNAscope Multiplex Fluorescent Reagent Kit V2	Biotechne	Cat. #: 323100	
Commercial assays	RNAscope probe against mouse musculus *Tbx15*	Biotechne	Cat. #: 558761	
Commercial assays	RNAscope intronic probe against mouse musculus *Myh4*	Biotechne	Cat. #: 539391-C3	
Commercial assays	RNAscope intronic probe against mouse musculus *Mybphl*	Biotechne	Cat. #: 1846041-C2	
Commercial assays	RNAscope H202 and Protease Reagents	Biotechne	Cat. #: PN 322381	
Commercial assays	RNAscope Target Retrieval reagents	Biotechne	Cat. #: 322000	
Commercial assays	RNAscope Wash buffer	Biotechne	Cat. #: PN 310091	
Commercial assays	TSA Vivid Fluorophore 570	R&D	Cat. #: 7526/1	
Commercial assays	TSA Vivid Fluorophore 650	R&D	Cat. #: 7527/1	
Commercial assays	RNAscope TSA Buffer	Biotechne	Cat. #: 322809	
Software, algorithm	Anaconda	Anaconda Inc.		
Software, algorithm	Big-FISH v. 0.6.2	10.1101/2021.07.20.453024		
Software, algorithm	Cellpose v. 3.1.0	10.1038/s41592-025-02595-5		
Software, algorithm	CellRanger v. 7.2.0	10X Genomics		
Software, algorithm	FiberSim v. 2.3.0	10.1016/j.bpj.2021.12.021		
Software, algorithm	FlowJo v. 10.8.2	Becton Dickinson		
Software, algorithm	ImageJ2 v. 2.16.0	NIH		
Software, algorithm	MyoProfiler	https://github.com/Campbell-Muscle-Lab/MyoProfiler		
Software, algorithm	Python v. 3.13.1	Python Software Foundation		
Software, algorithm	R v. 4.5.1	Rstudio		
Deposited data	Raw and analysed single nuclei RNA-sequencing data	This study	GEO: GSE322891	
Deposited data	Raw and analysed single nuclei multiome-sequencing data	This study	GEO: GSE322890	
Deposited data	Analysed mass-spectrometry data	This study	https://figshare.com/s/c786c35539d8cb212c31	
Bacterial and virus strain	AAV9-CK8-eGFP	This study, Vector Builder	Vector ID: VB250703-1475wrm	
Bacterial and virus strain	AAV9-CK8-mTbx15-eGFP	This study, Vector Builder	Vector ID: VB250120-1536jea	
Bacterial and virus strain	AAV9-CK8-mMybphl	This study, Vector Builder	Vector ID: VB251211-1415tqk	

Suppl. Table 3. Key resources table

Extended Data Table 1. (separate file)
Differentially expressed genes between EOM and TA myonuclei in sn-RNAseq.

Extended Data Table 2. (separate file)
Markers genes of EOM and TA myonuclear subpopulations in sn-RNAseq.

Extended Data Table 3. (separate file)
Markers genes of EOM, ILM and TA myonuclear subpopulation from sn-multiome.

Extended Data Table 4. (separate file)
Inference of putative Mybphl regulators. Peak, putative enhancer, peak_score, Spearman correlation between enhancer accessibility and target gene (single-cell level, average over significant tissues), peak_zscore, score corrected for accessibility (z-score against background peaks with similar accessibility, single-cell level, average over significant tissues), pct_peak, fraction of cells where peak was detected, tissue, tissues with significant enhancer-target association (pct_peak>0.01, z-score>1.5), tf, putative regulatory transcription factor, motif, motif of TF in JASPAR2024, motif_score, best motif score in enhancer, tf_peak_pooled, Spearman correlation between TF expression and enhancer accessibility (metacell-level, all tissues pooled), tf_peak_within, Spearman correlation between TF expression and enhancer accessibility (metacell-level, one correlation value per tissue, averaged), tf_target_pooled, Spearman correlation between TF expression and target expression (metacell-level, all tissues pooled), tf_peak_within, Spearman correlation between TF expression and target expression (metacell-level, one correlation value per tissue, averaged).

Extended Data Table 5. (separate file)

Regulon inference by Pando using the XGB method. Tf, transcription factor for which regulon was inferred, target, genes belonging to regulon, estimate, XGB score (sum of scores if multiple enhancers) for tf-enhancer-target association (higher is better), regions, putative enhancers in target vicinity (<100kb) containing transcription factor motif.